

Photographic documentation of astronomical observations has a long tradition. Since 30 years the development of CCD cameras has revolutionized acquisition and data processing of astronomical images. With the development of digital cameras for consumers, CCD cameras became also an important tool for amateur astronomers.

The fundamental problem in astronomical imaging is the limited number of photons which can be collected from the distant objects. Therefore long exposure times are required. For imaging of brighter objects like the moon or planets, the lucky imaging technique has been invented. At a very simplified basis, this method requires the acquisition of hundreds of single exposures. From these images only images which do not show any deformations due to atmospheric turbulences are selected for further processing. Stacking of these single images, which can have a very short exposure time, results in a sum image with rather long overall exposure time.

However, this technique cannot be applied to deep sky objects like nebulae or galaxies because the photon flux of these objects is way lower than for solar system objects. Just increasing the number of single exposures without increasing the single exposure time will not help because the signal produced on the CCD chip has to overcome the system noise of the camera electronics. Any signal below the system noise is lost after image read out and cannot be reconstructed by simple addition of many single exposures. Therefore, single exposures in the range of some minutes are required for deep sky imaging. Here EMCCD cameras offer a solution for this problem because their system noise is drastically reduced by the electron multiplication, enabling single exposure times in the second range.

For using lucky imaging for deep sky objects one has to keep in mind what lucky imaging really does. Apart from other effects lucky imaging reduces the point spread function of a point source to the theoretical value which is determined by the telescope aperture. This is achieved by reducing the probability that a single interfering effect affects the image quality via reduction of the exposure time. Then, in the second step of the lucky imaging process, only frames which are free of interfering effects are selected. What single exposure time is needed to make use of lucky imaging is defined by kind of interference, focal length and camera pixel size.

## Application Note

One factor in imaging is the correct sampling. According to the Nyquist theorem, in the ideal case the projection of a point source is spread as a Gaussian function over a square of 4-9 pixels. In the undersampling case the point spread function is smaller, in the oversampling case the point spread function is larger than this square. Thus correct sampling will harvest the optimal resolution of the camera chip. Concerning the undersampling case, as long as the broadening of the point spread function does not overcome the Nyquist theorem, this will not degrade the image quality, meaning that relatively long exposures are possible. In the oversampling case any broadening of the point spread function will reduce the image quality and has therefore to be avoided by shorter exposures.

The second important factor is the kind of air turbulences, the "seeing". It is often neglected that there are basically two types of seeing. One is caused by movements of big air volumes, which might cause aberrations of many arc seconds, but are slow, in the range of tenths of seconds. Thus choosing exposure times in the range of 1-10 seconds completely eliminates this problem. On the other hand, when exposure times of many minutes are needed for classical CCD cameras, this kind of seeing causes a catastrophic loss of image quality. The other kind of seeing is caused by fast micro turbulences which give rise to aberrations in the sub arc second range, but happen on timescales of less than one second. This type of seeing requires the very short exposure times used for the classical planetary lucky imaging with long focal lengths.

For this report, a Luca-R EMCCD camera from Andor Technology attached to a Celestron C9.25 Schmidt-Cassegrain telescope was used. The setup was mounted to a Skywatcher EQ6 mount without guiding control. For generation of color images mostly the LRGB technique was used, employing color filter sets of the company Baader Planetarium. The nominal focal length of the C9.25 (2350 mm) has been changed according to the object by using either focal reducer (1480 mm) or teleconverter lenses (4700 mm). For the Luca R camera with 8  $\mu\text{m}$  large pixels, the Nyquist theorem is fulfilled at focal lengths of about 4 meters. Focal lengths needed for most deep sky objects of interest for amateur astronomers are in the range of 1-4 meters, resulting in undersampled images. Therefore the single exposure time needed for deep sky lucky imaging can be rather long, in the range of some seconds.



## Application Note

For the focal lengths used in this report, usable exposure times and average disposal rates of bad frames can be seen in Tab. 1.

Focal length (mm)	Exposure time (sec)	Disposal rate (%)
1480	1	5
	5	10
	10	20
2350	1	10
	5	30
4700	1	40

The disposal rate does not correspond linearly to the exposure time since some disposal reasons are independent of the exposure time (planes, satellites, recentering of the object, ...).

One important feature of the short exposures is that no exact guiding control is required and even would have negative impact on picture quality. In order to avoid artifacts caused by pixel-to-pixel variations, each single frame has to be displaced compared to the frame before (dithering). Modern guiding software can be programmed to do this, but it is easier just to use no guiding at all. The mechanical errors of the mount then will perform the dithering automatically. The single raw images acquired at a first glance seem to be very noisy. Considering this, one has to keep in mind that only few photons reach the CCD chip during short exposure times. Thus, the noise in raw images is dominated by photon noise. A typical example is shown in Fig. 1a. After stacking (addition) of some hundred single exposures, a sum image with reasonable signal to noise ratio can be obtained (Fig. 1b).



Fig. 1a: Single raw frame of the planetary nebula Jones 1 in Pegasus. Exposure time was 10 sec.

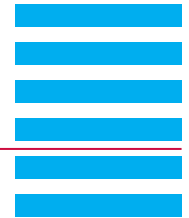


Fig. 1b: Stacked sum image of Jones 1. The color results from the combination of 1000 single frames of 10 sec each in the OIII band for green/blue and 1000 single frames in the H $\alpha$  band for red.

It should be noted that the Luca-R with the original factory setting is not suitable for astrophotography because the short clock time causes CME issues in low light conditions. Therefore, the clock time has to be

# Amateur astrophotography using the Luca-R EMCCD camera

C. Dosche, Oldenburg, Germany (May 2014)



## Application Note

changed to 11  $\mu$ s. However, this can be done within 5 minutes via remote maintenance. Another point which has to be considered when using EMCCD cameras is that for bright objects a kind of blooming effect happens in the amplification register. This causes electrons to bleed into the neighboring pixels, resulting in bad CME and smearing of bright objects. This effect can easily be seen in Fig. 2.



Fig. 2: Bicolor sum image of M27 resulting from overexposed single frames, showing the smear effect in the EM register

The only way to avoid this is to reduce the single exposure time as far as possible. In general, the exposure time can be reduced almost freely, the only condition is that at least two stars remain visible for control of image quality and orientation.

Examples of astronomical images taken with the Luca-R can be found in the appendix. In mid European conditions, normally resolutions of about 1 arc second and magnitudes of  $\sim 21$  m can be reached by using EMCCD lucky imaging. In summary, the Luca-R camera platform offers a very interesting alternative to established imaging setups because it allows to harvest the full theoretical resolution of common telescope apertures and, as no guiding is necessary, enables highly mobile imaging, which has become more and more important in the age of light pollution.

### Contact

Dr. Carsten Dosche  
Institute of Chemistry  
Carl von Ossietzky University Oldenburg  
Carl-von-Ossietzky-Str. 9-11  
26129 Oldenburg  
Germany

Phone: +49 (441) 798-3975

E-mail: [carsten@dosche.de](mailto:carsten@dosche.de)

Web: <http://junior-ccd.fn-f.de/>  
[www.naa.net](http://www.naa.net)

# Amateur Astrophotography using the Luca R EMCCD camera

## - Appendix -

### 1. Galaxies



Fig. 1: M81, Bode's Galaxy in Ursa Major,  
1480 mm, RGB 3x1000x2 sec



Fig. 2: M82 in U. Major, with SN2014J  
2350 mm, RGB 3x1000x1.5 sec



Fig. 3: M65 in Leo,  
1480 mm, RGB 3x500x5 sec



Fig. 4: NGC 2903 in Leo,  
1480 mm, LRGB, L: 1500x5 sec,  
RGB: 3x1000x5 sec





Fig. 5: NGC 3718 in Ursa Major,  
1480 mm, LRGB, L: 1000x5 sec,  
RGB: 3x500x5 sec



Fig. 6: Hickson 44 galaxy group in Leo,  
1480 mm, LRGB, L: 1000x5 sec,  
RGB: 3x500x5 sec

## 2. Galactic Nebulas



Fig. 7: M20 (Trifid Nebula) in Sagittarius,  
1480 mm, RGB 3x750x2 sec



Fig. 8: M17 (Omega Nebula) in Sagittarius,  
2350 mm, Ha/OIII: 2x1000x2 sec



Fig. 9: Barnard 33 (Horsehead Nebula) in Orion,  
1480 mm, LRGB, L: 500x5 sec,  
Ha,OIII,Hb 3x500x2 sec



Fig. 10: M42 (Orion Nebula) in Orion,  
1480 mm, RGB 3x500x1 sec



Fig. 11: NGC 6888 (Crescent Nebula) in Cygnus,  
1480 mm, Ha/OIII: 2x1000x2 sec



Fig. 12: NGC 7023 (Iris Nebula) in Cepheus,  
1480 mm, RGB 3x1000x5 sec





Fig. 13: IC 5146 (Cocoon Nebula) in  
Cygnus,  
1480 mm, RGB 3x1000x2 sec



Fig. 14: Cygnus supernova remnant,  
1480 mm, Ha/OIII: 2x1000x5 sec

### 3. Globular Clusters



Fig. 15: M13 in Hercules,  
1480 mm, LRGB, L: 1000x0.75sec,  
RGB: 3x1000x0,75 sec



Fig. 16: M22 in Sagittarius,  
1480 mm, RGB 3x1000x1 sec

## 4. Planetary Nebulas



Fig. 17: M97 (Owl Nebula) in Ursa Major,  
1600 mm, Ha/OIII 2x500x10 sec



Fig. 18: Abell 21 (Medusa Nebula) in  
Gemini,  
1480mm, 850x10 sec (Ha),  
500x10 sec (OIII)

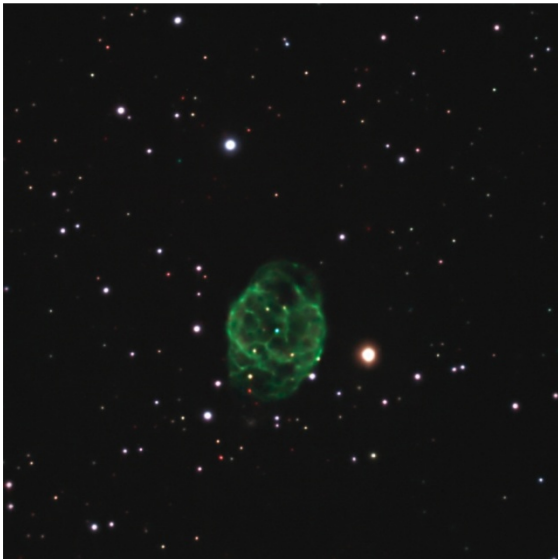


Fig. 19: Abell 72 in Dolphin,  
2350 mm, Ha/OIII 2x750x10 sec



Fig. 20: NGC 7293 (Helix Nebula) in  
Aquarius,  
1480 mm, LRGB, L: 750x5 sec,  
RGB: 3x750x5 sec





Fig. 21: Jones 1 in Pegasus,  
1480 mm, Ha/OIII 2x1000x10 sec

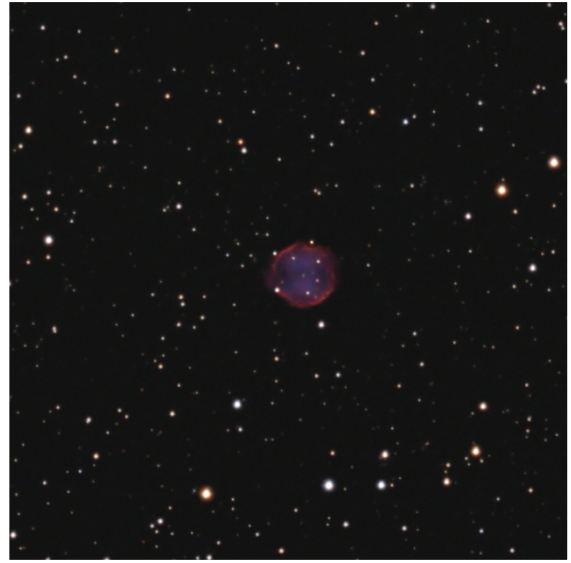


Fig. 22: NGC 7139 in Cepheus,  
3000 mm, RGB 3x1000x2 sec



Fig. 23: NGC 6765 in Lyra,  
3000 mm, RGB 3x1000x2 sec



Fig. 24: PK 080-06.1 (Egg Nebula) in  
Cygnus,  
4700 mm, RGB 3x1000x2 sec